RESEARCH ARTICLE
Legume Research- An International Journal, Volume 45 Issue 3: 319-326 (March 2022)

Rabi Groundnut Area Estimation using Synthetic Aperture Radar (SAR) in Thiruvannamalai District of Tamil Nadu

S. Thirumeninathan[1], S. Pazhanivelan[2], N.S. Sudarmanian[2],
K.P. Ragunath[2], A. Gurusamy[3], N. Sritharan[4]

10.18805/LR-4746

ABSTRACT

Background: Groundnut, commonly known as peanut, is a significant oil, food and feed legume crop grown in all seasons in Tamil Nadu, including *kharif, rabi* and *summer* and it is cultivated both under irrigated and rainfed conditions in all the seasons at Thiruvannamlai district. One of the most important applications of remote sensing in agriculture is a crop acreage and production estimation (CAPE). The CAPE's main goal is to estimate crop acreage and production of important crops, so that advanced food production, distribution and supply data were achieved.

Methods: Multi-temporal Sentinel 1A SAR IW- GRD data with 20 m spatial resolution and 12 days temporal resolution of vertical - horizontal (V-H) polarization were downloaded for the period of 4th October 2020 to 8th January 2021 to have the full coverage during the crop growth period in the study area used for this work. Crop backscattering and multi-temporal features were extracted from MAPscape 5.2 automated pre-processing tool and its classified using supervised maximum likelihood classification for groundnut acreage extraction for Thiruvannamalai district.

Result: The *rabi* groundnut area of Thiruvannamalai district of Tamil Nadu was estimated using SAR Sentinel-1A data as 32298 ha with a higher accuracy percentage of 87.4 and kappa coefficient of 0.75.

Key words: Backscattering, Groundnut, MAPScape, Maximum likelihood classification, Multi-temporal features, QGIS, Sentinel-1A.

INTRODUCTION

Groundnut (*Arachis hypogaea* L.) is predominant oilseed crop grown in tropical and subtropical climates around the world. It is grown in different rainfall and temperature regimes on a variety of soils. India occupied the second position in acreage and production of groundnut with an area of 3.35 million hectares and a production of 9.11 million tonnes with an average productivity of 2720 2720 kg ha^{-1} during 2018-19 (Directorate of Economics and Statistics, 2020).

In Tamil Nadu, it is the major oilseed crop grown under rainfed and irrigated condition accounting for 5.7% of the total cropped area. Groundnut is grown on an area of 3.35 lakh hectares with a production of 9.11 lakh tonnes during 2018-19 in the state (Directorate of Economics and Statistics, 2020). The districts *viz.*, Tiruvannamalai, Vellore, Villupuram, Namakkal, Erode and Salem constituted 54.9% of the area under groundnut in Tamil Nadu.

In general, crop cultivated area is estimated using agricultural statistics obtained from field visits and interview with the farmers, which is extremely tedious, time-consuming, labour intensive, less precise, expensive, inconsistent and too generalized (Prasad *et al.*, 2006). It is, however unable to provide timely information on regional spatial distribution of crop growing areas. One of the most common uses of remote sensing in agriculture is crop acreage and production estimation (CAPE). The prime objective of CAPE is the estimation of crop acreage and production of major crops to assist advanced planning for food production, distribution and supply. The remote sensing approach has the ability to provide information on agricultural crops quantitatively, instantaneously and above all, non-destructively over broad areas. Crop phenological information data can also derived through remote sensing (Karnieli, 2003 and Xin *et al.*, 2002).

In crop production, crop acreage is the most important component. Crop acreage must be monitored and estimated on a national scale in order to evaluate the national, regional food demand and supply balance, as well as to assess social security. Veloso *et al.* (2017) reported that crop mapping and estimation of biophysical parameter using SAR backscatter and NDVI temporal behaviors would help better

[1]Department of Agronomy, Tamil Nadu Agricultural University, Coimbatore-641 003, Tamil Nadu, India.
[2]Department of Remote Sensing and GIS, Tamil Nadu Agricultural University, Coimbatore-641 003, Tamil Nadu, India.
[3]Dryland Agricultural Research Station, Tamil Nadu Agricultural University, Coimbatore-641 003, Tamil Nadu, India.
[4]Department of Crop Physiology, Tamil Nadu Agricultural University, Coimbatore-641 003, Tamil Nadu, India.

Corresponding Author: S. Thirumeninathan, Department of Agronomy, Tamil Nadu Agricultural University, Coimbatore-641 003, Tamil Nadu, India. Email: thirumeni95@gmail.com

How to cite this article: Thirumeninathan, S., Pazhanivelan, S., Sudarmanian, N.S., Ragunath, K.P., Gurusamy, A. and Sritharan, N. (2022). *Rabi* Groundnut Area Estimation using Synthetic Aperture Radar (SAR) in Thiruvannamalai District of Tamil Nadu. Legume Research. 45(3): 319-326. DOI: 10.18805/LR-4746.

Submitted: 20-07-2021 **Accepted:** 10-11-2021 **Online:** 16-12-2021

understanding of agricultural activities and environmental conditions.

Crop identification, discrimination and early estimation are essential for planning delivery estimates, harvest and storage needs. However, operations that rely entirely on optical images for productivity and yield monitoring are subjected to data gaps during critical crop growth stages due to clouds and haze have little effect on SAR. SAR data also give complementary and unique characterizations of vegetation due to its sensitivity to canopy geometry as compared to the information provided by optical image, in addition to this of tested advantage (Jia *et al.,* 2012). According to Haldar *et al.* (2017) due to volume scattering that as the plant develops the RADAR backscatter increases as plant grows. Cotton and groundnut crops are detected and discriminated from the other major land covers using a decision rule-based model and the use of multi temporal SAR data appears to be promising, crop backscattering is dynamic during the growth stage. During cloudy and rainy conditions, image collection is limited due to optical sensor relies on solar light. As a result the remote sensing system that can work in all weather conditions.

Radar has a great potential to provide information in such a manner. Previous studies have shown that SAR images have a lot of potential of crop acreage and monitoring (McNairn *et al.,* 2013). Furthermore, the accuracy of crop classification is not always as good as required for better decision making given the current state of the art of SAR imagery interpretation methodologies. To improve crop identification and area estimation, there is need to have a better understanding of the crop and the underlying soil characteristics that influence radar backscatter throughout the growing season, to find a suiTable methodology to extracting crop information from SAR imagery and to evaluate the multi temporal SAR data for crop identification.

MATERIALS AND METHODS

Study area

Thiruvannamalai district comes under North Eastern Agro Climatic Zones of Tamil Nadu with the spread over of 6191 square kilometers. It lies between 11° 55′ to 13° 15′ North latitude and 78° 20′ to 79° 50′ East longitude. This district has eighteen blocks consisting of 1067 revenue villages and study area map were presented in Fig 1. The climate is hot sub humid to semi-arid. The mean annual maximum and minimum temperature are 32.6 and 22.2°C, respectively. The annual rainfall of the North Eastern Zone excluding hills varied from 800-1400 mm. Predominant soil type was red sandy loam and clay loam soil, which encourages the cultivation of groundnut, rice, blackgram and sessame. The experiment was conducted at Department of Remote Sensing and GIS, Tamil Nadu Agriculture University, Coimbatore, Tamil Nadu during *rabi* season 2020-21.

Data used

Synthetic aperture radar (SAR) has the advantage of operating at wavelengths not impeded by cloud cover or lack of illumination and can acquire data over a site during day or night time. Sentinel 1A, with its C-SAR instrument can offer reliable, repeated wide area monitoring. The Sentinel 1 mission includes C-band imaging system operating in four imaging modes with different resolutions and area coverage. It provides dual polarization capability, short revisit period and rapid product delivery. Ground range detected (GRD) and single look complex (SLC) datasets from Sentinel 1A Synthetic Aperture Radar imaging system with VV and VH polarizations in Interferometric Wide (IW) swath mode are obtained at 12 days interval and used for crop identification and mapping in the study area. Based on the normal growing season of groundnut in the study area, the data were downloaded from https://scihub.copernicus.eu/

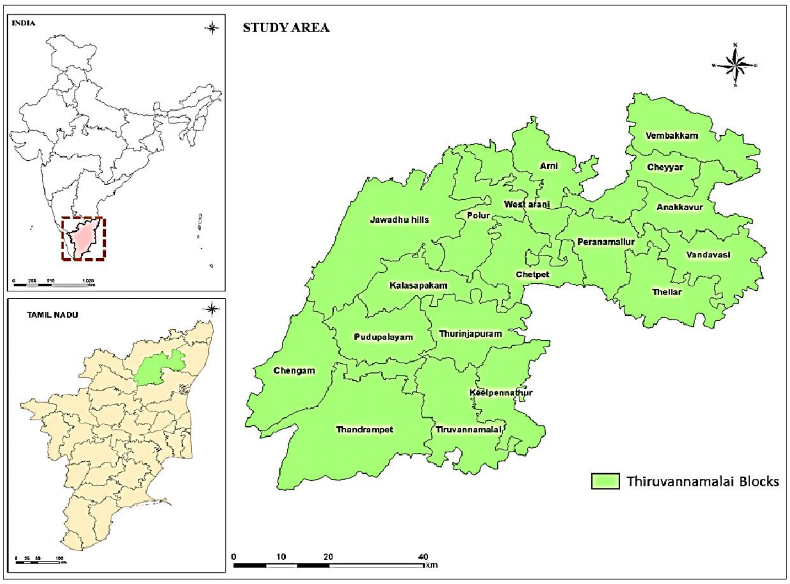

Fig 1: Study area map of Thiruvannamalai district from Tamil Nadu.

dhus/ for the period of 4th October 2020 to 8th January 2021 to have the full coverage during the crop growth period in the study area.

Ground truth collection

Ground truth points were collected during *Rabi* 2020-21 in the groundnut growing areas of the study area at different crop growth stages and the crop calendar were presented in Fig 3, 4. Totally 103 groundnut points and 34 other crop points were collected during the ground survey for training and validation using random stratified sampling method.

SAR data processing

A fully automated processing chain developed by Holecz *et al.*, (2013) was used to convert the multi-temporal space-borne Sentinel 1A SAR IW-GRD data into terrain-geocoded σ° values. The processing chain was a module within the MAPscape-RICE software, developed by *sarmap*, Switzerland. The SAR time-series data underwent a series of basic processing steps to generate terrain-geocoded σ° values as detailed below and presented in Fig 2.

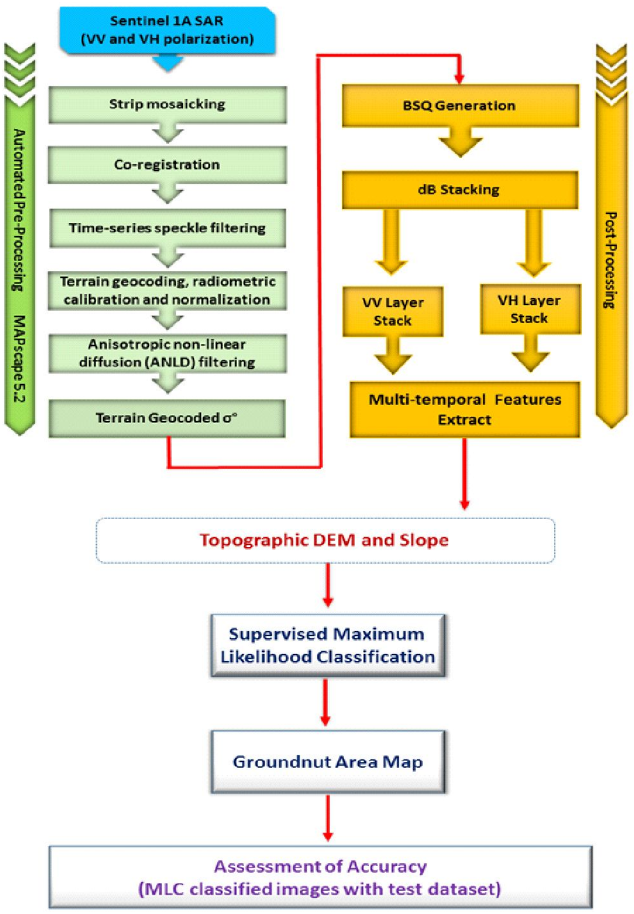

Fig 2: Flow chart depicting the methodology of SAR data processing and area mapping.

(i) Strip mosaicking

To facilitate the overall data processing and data handling.

ii) Co-registration

Images acquired with the same observation geometry were co registered in slant range geometry.

iii) Time-series speckle filtering

To balance differences in reflectivity between images.

iv) Terrain geocoding

Radiometric calibration and normalization.

v) ANLD filtering

To get smoothened homogeneous targets.

vi) Removal of atmospheric attenuation

σ° values were corrected by means of an interpolator.

vii) Subsetting

The rectangular extent of the study was extracted from the base map and the raster images were subsetted to an extent from 11° 55′ to 13° 15′ North latitude and 78° 20' to 79° 50' East longitude. Subsetting of raster data reduces the time in further processing.

Multi-temporal feature extraction

Multi-temporal features *viz*., minimum, maximum, mean, minimum date, maximum date and span ratio of VV, VH polarizations and minimum, maximum and mean features of coherence (cc) data were extracted using feature extraction tool in MAPscape-RICE software. These multi-temporal features are having certain range regarding groundnut crop, which were extracted using point sampling tool of QGIS 3.20.0.

Crop classification

The aim of the image classification is to categorize the image pixels into a land cover category based on the pixel value. This section explains the classification methodology used in this study for groundnut crop area identification and classification.

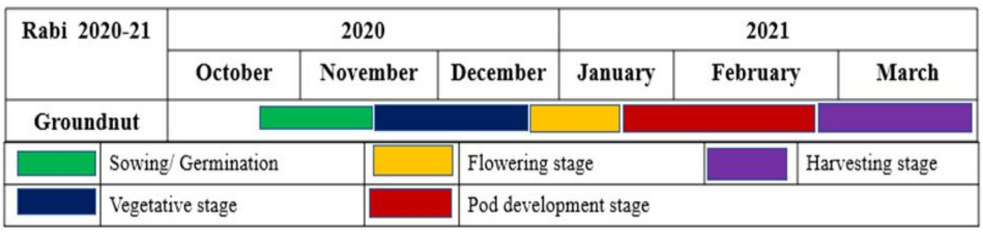

Fig 3: Groundnut crop calendar during *rabi* 2020-21.

Maximum likelihood classification (MLC)

Maximum likelihood classification (MLC) algorithm was used in this study for crop area identification. The MLC quantitatively evaluates both the variance and covariance of the category by spectral response pattern when classifying an unknown pixel. Class mask (containing different classes) generated using multi temporal features of groundnut fields for both VH and VV polarization images in study area were used in the classification. The class mask file was used to precisely segregate the groundnut pixels from other class pixels.

Accuracy assessment

The error matrix and Kappa statistics are used for evaluating the classification accuracy. The class allocation of each pixel in classified image is compared with the corresponding class allocation on reference data to determine the classification accuracy. The ground reference data are used for validation and the pixels of agreement and disagreement are compiled in the form of an error matrix. The accuracy measures such as overall accuracy, producer's accuracy and user's accuracy are estimated. Kappa coefficient is another measure of classification accuracy. It is a measure of the proportional improvement by the classifier over a purely random assignment to classes.

RESULTS AND DISCUSSION

Radar backscattering signature

SAR data have a proven ability to detect groundnut through the unique temporal signature of the backscatter coefficient (also termed sigma naught - σ°) exhibited by the crop. The radar backscattering coefficient (σ°) is a measure of crop biomass, plant height, water content, underlying soil, crop phenology *etc*. The SAR data collected during the cropping period was processed and analyzed using training pixels from ground truth points to derive the temporal backscattering coefficient (σ°) for groundnut from the study area. The temporal backscattering signatures of groundnut during *rabi* 2020-21 were generated by stacking nine SAR acquisitions from 4th October 2020 to 8th January 2021. The signature curves of mean backscattering (dB) values for groundnut showed a marginal increase in backscattering at seedling to vegetative stage (D_1 to D_3) and a steep increase from flowering to pod development stage (D_4 to D_6) followed by a decline thereafter at maturity (D_7 to D_9) and it will present in Table 1 and Fig 4a, 4b. Temporal backscatter values were recorded in 25 test sites across Thiruvannamalai districts and the details are presented in Table 2 and Fig 4c. In that district, backscattering values were found to be ranging from -19.22 to -15.57 dB and -19.37 to -15.50 dB at D_1 (16th October 2020) and D_2 (28th October 2020) in VH polarization. At D_4 corresponding to flowering and peg penetration stage, the values were -18.79 to -15.06 dB. The backscattering values increased further and reached a maximum of -18.44 to -14.62 dB and -19.59 to 15.10 at D_6 and D_7 corresponding to pod development to maturity stages and declined thereafter. The increased backscattering values at initial growth stages to flowering stages primarily influenced by LAI and biomass of the crop (Deiveegan *et al.,* 2016) and decrease in backscatter values at the later stages might have been probably caused by maturity of the crop, which lowered the water content of the vegetation or related to the vegetation biomass and or related to the reduced volumetric scattering due to maturity (Panigrahy and Mishra, 2003).

Multi temporal features extraction

Temporal signatures were extracted for each monitoring site and used to generate the dB curves for groundnut fields shows the temporal signature for selected representative pixels to visualize the resulting maximum likelihood classification using multi temporal features (MTF) from C-band SAR imagery of Sentinel-1A. The multi temporal features (in dB value) *viz.* max, min, mean, max date, min date and span ratio were generated using nine acquisitions during *rabi* 2020-21 and presented in Table 2. Among the features, the max feature *i.e.* maximum value for different monitoring fields of groundnut ranged from -19.23 to -15.57 at VH Polarization. Min feature *i.e.* minimum value ranged from -19.86 to -16.77 at VH polarization. Similarly, mean *i.e.* mean value and span ratio for groundnut fields are ranged from -18.29 to -15.39 and 2.15 to 5.10, respectively at VH polarization. In groundnut fields of Tiruvannamalai districts, the max date features for VH polarization was recorded at D_9 (8th January 2021). The min date feature for VH polarization was recorded between D_1 (4th October 2020) and D_3 (28th October 2020) with majority of the fields recording minimum date as D_2 (16th October 2020). SAR based C band imageries of Sentinel 1A were used to generate information of groundnut, which was in line with the findings of Nelson *et al.* (2014), they were used SAR sensors at short wavelengths in the bands of X, C, K_a and K_u at greater incident angles are suitably sensitive to detect even tiny seedlings immediately after emergence. Whereas, Venkatesan *et al.* (2019) used microwave SAR Sentinel data for multi temporal features extraction on maize crop at Pereambalur and Ariyalur district of Tamil Nadu.

Groundnut area and accuracy

Groundnut area map for the Thiruvannamalai district were derived from multi temporal C-band SAR imagery of

Table 1: Mean temporal backscattering (dB) values for monitoring sites of groundnut during *rabi* 2020-21.

Satellite pass	Date of passing	Mean dB
D_1	04.10.2020	-17.60
D_2	16.10.2020	-18.11
D_3	28.10.2020	-17.91
D_4	09.11.2020	-17.21
D_5	21.11.2020	-16.61
D_6	03.12.2020	-15.81
D_7	09.12.2020	-15.69
D_8	15.12.2020	-16.13
D_9	08.01.2021	-14.63

Sentinel-1A. Using the shape files of administrative boundaries, district wise and block wise maps and statistics of groundnut area were extracted for 18 blocks of Thiruvannamalai district. The classified groundnut area for the blocks and district were presented in the Table 3. The total groundnut growing area during *rabi* 2020-21 at Thiruvannamalai district was classified as 32298 ha. Among the blocks of Thiruvannamalai district, Thandrampet block recorded maximum area of 6970 ha and followed by Thurinjapuram, Thiruvannamalai, Keelpennathur and

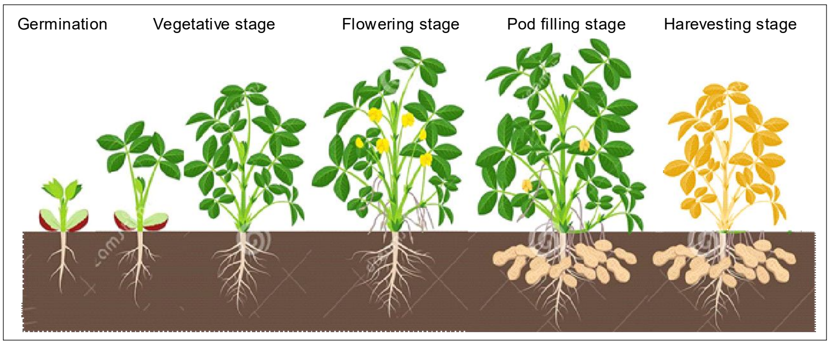

Fig 4a: Groundnut growth stages.

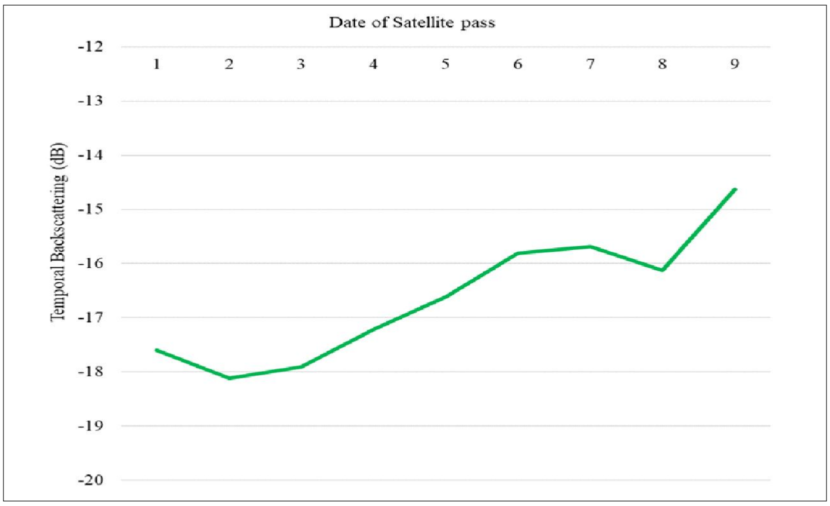

Fig 4b: Mean temporal backscattering curve (dB).

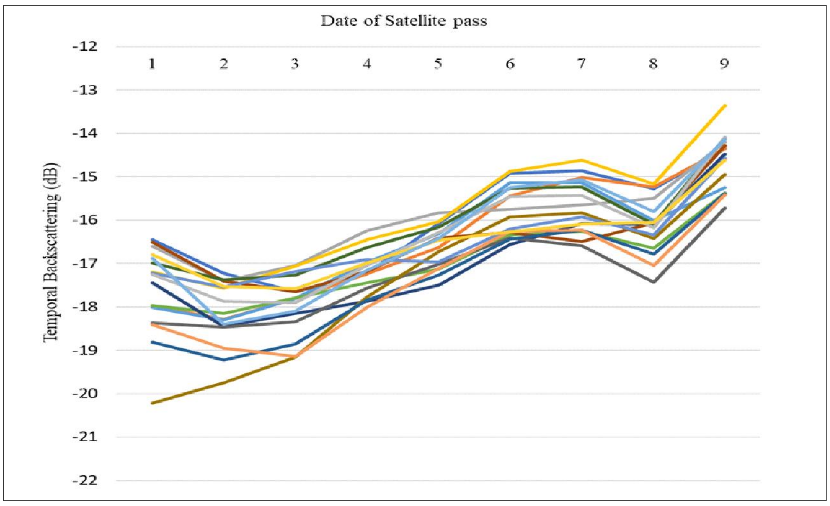

Fig 4c: Temporal backscattering (dB) curve for monitoring sites.

Table 2: Temporal backscattering (dB) values and VH polarisation multi temporal features for monitoring sites of groundnut fields in Thiruvannamalai district during *rabi* 2020-21.

		Temporal backscattering (dB) values									VH Polarisation - Multi temporal features					
Long.	Lat.	D_1	D_2	D_3	D_4	D_5	D_6	D_7	D_8	D_9	Max	Min	Mean	Max_D	Min_D	SpanRat
79.26	12.77	-17.8	-18.4	-18.7	-18.2	-17.3	-15.8	-16.1	-16.9	-15.9	-15.8	-18.7	-16.9	11	8	3.0
79.33	12.67	-16.5	-17.2	-17.7	-17.2	-16.1	-14.9	-14.9	-15.3	-14.4	-14.2	-17.7	-15.5	1	8	3.4
79.20	12.56	-16.5	-16.8	-16.3	-15.9	-16.0	-15.9	-15.9	-15.9	-14.6	-14.6	-16.8	-15.8	14	7	2.2
79.25	12.48	-18.0	-18.3	-17.8	-17.2	-16.6	-15.5	-15.0	-15.2	-14.4	-14.4	-18.3	-16.0	14	7	3.9
79.16	12.44	-16.6	-17.4	-17.0	-16.3	-15.8	-15.7	-15.7	-15.5	-14.2	-14.2	-17.4	-15.8	14	7	3.2
79.20	12.39	-17.2	-17.6	-17.1	-16.5	-16.0	-14.9	-14.6	-15.2	-13.4	-13.4	-17.6	-15.4	14	7	4.2
78.93	12.40	-18.0	-18.2	-17.8	-17.5	-17.1	-16.3	-16.3	-16.6	-15.4	-15.4	-18.2	-17.0	14	7	2.8
79.18	12.26	-17.5	-18.5	-18.2	-17.9	-17.5	-16.6	-16.1	-16.1	-14.5	-14.5	-18.5	-16.7	14	7	4.0
79.47	12.57	-15.9	-16.2	-16.3	-16.0	-15.7	-16.9	-18.5	-17.0	-14.7	-14.5	-18.5	-16.1	1	12	4.0
79.50	12.58	-16.5	-17.4	-17.7	-17.2	-16.4	-16.3	-16.5	-16.1	-14.3	-14.3	-17.7	-16.3	14	8	3.4
78.93	12.19	-18.0	-18.7	-18.2	-17.6	-17.4	-17.2	-17.1	-17.4	-14.8	-14.8	-18.7	-17.1	14	7	3.9
79.02	12.12	-17.7	-17.9	-18.0	-17.6	-17.3	-17.0	-17.4	-18.1	-15.9	-15.9	-18.1	-17.3	14	13	2.2
79.01	12.11	-18.4	-18.5	-18.3	-17.6	-17.0	-16.4	-16.6	-17.4	-15.7	-15.7	-18.6	-17.6	14	3	2.9
79.03	12.10	-20.2	-19.7	-19.2	-17.8	-16.7	-15.9	-15.8	-16.4	-14.9	-14.9	-20.2	-17.7	14	6	5.3
79.00	12.08	-18.7	-18.7	-18.5	-18.1	-17.8	-16.8	-16.9	-17.9	-15.5	-15.5	-19.7	-18.0	14	3	4.2
79.16	12.40	-18.8	-19.2	-18.9	-17.9	-17.3	-16.4	-16.2	-16.8	-15.4	-14.9	-19.2	-17.1	1	7	4.3
79.22	12.40	-17.0	-17.4	-17.3	-16.6	-16.2	-15.3	-15.2	-16.1	-14.1	-14.1	-17.4	-15.9	14	7	3.3
79.19	12.34	-17.2	-17.6	-17.2	-16.9	-17.0	-16.2	-15.9	-16.3	-14.6	-14.6	-17.6	-16.2	14	7	3.0
79.14	12.36	-18.4	-19.0	-19.1	-18.0	-17.1	-16.3	-16.2	-17.0	-15.4	-15.4	-19.1	-17.3	14	8	3.7
79.14	12.37	-17.3	-17.9	-17.9	-17.1	-16.3	-15.5	-15.4	-16.2	-14.1	-14.1	-17.9	-16.1	14	8	3.8
79.08	12.32	-16.0	-16.3	-16.4	-16.1	-15.8	-15.0	-14.7	-15.1	-14.0	-14.0	-16.8	-15.6	14	3	2.9
79.13	12.25	-16.9	-18.4	-18.1	-17.2	-16.4	-15.3	-15.1	-15.8	-14.1	-14.1	-18.4	-16.2	14	7	4.3
79.17	12.10	-18.3	-18.5	-18.5	-18.4	-17.4	-15.8	-15.8	-16.7	-15.5	-15.5	-18.5	-17.0	14	7	3.1
79.18	12.13	-17.1	-18.6	-18.5	-18.4	-16.9	-14.6	-14.4	-15.2	-13.6	-13.6	-18.6	-15.9	14	7	5.0
79.33	12.60	-17.5	-18.5	-18.9	-18.7	-17.3	-15.8	-15.9	-16.5	-15.3	-14.5	-18.9	-16.3	1	8	4.3

Table 3: Block-wise groundnut area for Thiruvannamalai district during *rabi* 2020-21.

Name	Groundnut area (ha)
Vembakkam	36
Arni	220
West arani	421
Polur	216
Cheyyar	171
Jawadhu hills	29
Anakkavur	57
Peranamallur	491
Chetpet	454
Vandavasi	328
Thellar	103
Kalasapakam	757
Thurinjapuram	5576
Pudupalayam	2173
Chengam	4111
Keelpennathur	4989
Tiruvannamalai	5197
Thandrampet	6970
Total	32298

Chengam blocks with 5576, 5197, 4989 and 4111 ha, respectively. The minimum area of 29 ha was recorded at Jawadhu hills block of Thiruvannamalai district (Fig 5).

The accuracy assessment for the groundnut area maps was conducted on a groundnut or non-groundnut basis, where all other land cover types were grouped into single non-groundnut class. In total, 103 validation points covering 69 groundnut and 34 non-groundnut points were considered for validation and confusion matrix were presented in Table 4. The overall classification accuracy was 87.4 per cent with a kappa score of 0.75 indicating the accuracy of classification. The overall accuracy (>80) and kappa index (>0.50) indicated that good level of assessment. The high accuracy of classification in the study area demonstrated that the methodology was appropriate for groundnut area estimation using multi-temporal Sentinel 1A data and indicated the suitability of these remote sensing-based products for policy decisions including crop insurances as quoted by Deiveegan *et al.* (2016). The findings were in line with Venkatesan *et al.* (2019) estimated maize area with an accuracy of 91 per cent and Sudarmanian *et al.* (2017) estimated rice area of Thiruchirapalli district of Tamil Nadu with an high accuracy and quantify the methane emission from paddy field using remote sensing datasets.

Table 4: Confusion matrix for accuracy assessment for groundnut classification during *rabi* 2020-21.

Actual class from survey	Predicted class from the map			
		Groundnut	Non-groundnut	Accuracy (%)
	Groundnut	59	10	85.5
	Non-groundnut	3	31	91.2
	Reliability (%)	95.2	75.6	87.4
	Average accuracy		88.3%	
	Average reliability		85.4%	
	Overall accuracy		87.4%	Good accuracy
	Kappa index		0.75	Good accuracy

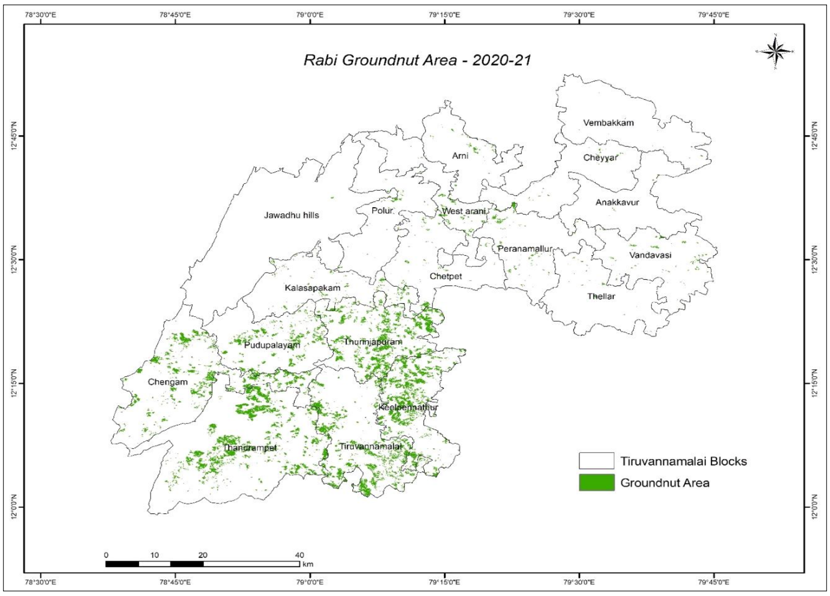

Fig 5: Groundnut area map of Thiruvannamalai district during *rabi* 2020-21.

CONCLUSION

The *rabi* groundnut area estimated using SAR Sentinel-1A data by supervised maximum likelihood classification and thorough analysis of temporal backscattering during crop growth stages. The estimated groundnut area was 32298 ha with a higher accuracy percentage of 87.4 and kappa coefficient of 0.75.

ACKNOWLEDGEMENT

The authors thank the Agriculture and Land Eco System Division, Space Application Centre, ISRO, Ahmedabad for providing the fund to carry out the research work in a project mode (Space Technology Utilization for Food Security, Agricultural Assessment and Monitoring-SUFALAM Project) and also thank the Professor and Head and staff of the Department of Remote Sensing and GIS, TNAU for their valuable comments and constructive suggestions on the manuscript.

REFERENCES

Deiveegan, M., Pazhanivelan, S., Ragunath, K. and Kumaraperumal, R. (2016). Detection of Agricultural vulnerability to drought using NDVI and Land Surface Temperature in Salem and Namakkal districts of Tamil Nadu. Advances in Life Sciences. 5: 6868-6873.

Directorate of Economics and Statistics (DES), (2020). Agricultural Statistics at a Glance. Department of Agriculture and Co-Operation. Ministry of Agriculture, Government of India. Available online: http://eands.dacnet.nic.in (Accessed on 20th April, 2021).

Halder, D., Panda, R.K., Srivastava, R.K. and Kheroar, S. (2017). Evaluation of the CROPGRO-Peanut model in simulating appropriate sowing date and phosphorus fertilizer application rate for peanut in a subtropical region of eastern India. The Crop Journal. 5: 317-325.

Holecz, F., Barbieri, M., Collivignarelli, F., Gatti, L., Nelson, A., Setiyono, T.D., Boschetti, M., Manfron, G., Brivio, P.A., Quilang, J.E. and Obico, M.R. (2013). An Operational Remote Sensing based Service for Rice Production Estimation at National Scale. In Proceedings of the Living Planet Symposium. Edinburgh, United Kingdom: ESA.

Jia, K., Li, Q., Tian, Y., Wu, B., Zhang, F. and Meng, J. (2012). Crop classification using multi-configuration SAR data in the North China Plain. International Journal of Remote Sensing. 33: 170-183.

Karnieli, A. (2003). Natural vegetation phenology assessment by ground spectral measurements in two semi-arid environments. International Journal of Biometeorology. 47: 179-187.

McNairn, H., Champagne, C., Shang, J., Holmstrom, D. and Reichert, G. (2009). Integration of optical and synthetic aperture radar (SAR) imagery for delivering operational annual crop inventories. ISPRS Journal of Photogrammetry and Remote Sensing. 64: 434-449.

Nelson, A., Setiyono, T., Rala, A.B., Quicho, E.D., Raviz, J.V., Abonete, P.J., Maunahan, A.A., Garcia, C.A., Bhatti, H.Z.M., Villano, L.S. and Thongbai, P. (2014). Towards an operational SAR-based rice monitoring system in Asia: Examples from 13 demonstration sites across Asia in the RIICE project. Remote Sensing. 6: 10773-10812.

Panigrahi, R.K. and Mishra, A.K. (2013). Unsupervised classification of scattering behaviour using hybrid-polarimetry. IET Radar, Sonar and Navigation. 7: 270-276.

Prasad, A.K., Chai, L., Singh, R.P. and Kafatos, M. (2006). Crop yield estimation model for Iowa using remote sensing and surface parameters. International Journal of Applied Earth Observation and Geoinformation. 8: 26-33.

Sudarmanian, N.S., Pazhanivelan, S. and Ragunath, K.P. (2017). Remote Sensing based Methane Emission from Rice fields in Tiruchirapalli District. Madras Agriculture Journal. 104(4-6): 175-178.

Veloso, A., Mermoz, S., Bouvet, A., Le Toan, T., Planells, M., Dejoux, J.F. and Ceschia, E. (2017). Understanding the temporal behavior of crops using Sentinel-1 and Sentinel-2-like data for agricultural applications. Remote Sensing of Environment. 199: 415-426.

Venkatesan, M., Pazhanivelan, S. and Sudarmanian, N.S. (2019). Multi-temporal feature extraction for precise maize area mapping using time-series Sentinel 1A SAR data. The International Archives of the Photogrammetry, Remote Sensing and Spatial Information Sciences, Volume XLII-3/W6. DOI:10.5194/isprs-archives-XLII-3-W6-169-2019.

Xin, J., Yu, Z., van Leeuwen, L. and Driessen, P.M. (2002). Mapping crop key phenological stages in the North China Plain using NOAA time series images. International Journal of Applied Earth Observation and Geoinformation. 4: 109-117.